Quantification of Image Quality

Pong Wing Tat*, Alfred Wong**, Department of Electrical and Electronic Engineering, University of Hong Kong, Hong Kong

ABSTRACT

Traditionally, the common window method is used to quantify image quality in optical lithography. The common window method can take dose variation, focus error, mask critical dimension error and aberrations into account. However, the demerit of the common window method is its computation time. In this paper, a new metric called Normalized Process Latitude (NPL) is proposed. The NPL considers dose variation, focus error, mask critical dimension error and aberrations to output its final quantification value. Its processing time for quantifying one feature is usually within 10 seconds on a PC with 1GHz CPU and 256MB DRAM. We perform several comparisons between the total window value and the NPL. It is found that the NPL draws similar conclusion as the total window. We can conclude that NPL is a sensible figure of merit for image quantification.

Keywords: normalized process latitude, normalized image log slope, mask error factor, chromium-on-glass (COG), aberrations, sigmoid function, ED window, extraction, normalization, combination

1. INTRODUCTION

As the k1 factor decreases continuously, optical images are ever more sensitive to fluctuations and nonidealities of the exposure process. Exposure latitude and depth-of-focus have traditionally been used as metrics to quantify the sensitivity of optical images to dose and focus nonuniformities. With the increasing contributions by mask errors and aberrations to linewidth variability, there is a need to quantify image sensitivity to these sources of linewidth error as well. The mask error factor [1,2] and depth-of-aberrations [3] are example metrics. However, it is sometimes desirable to represent the robustness of an image by a single number that contains information on sensitivities to dose, focus, mask error, and aberrations. The ED window [4] method takes into consideration the robustness of an image against focus and dose variations. This method can be extended to accommodate mask errors and aberrations by overlapping various ED windows to form a common window [5,6]. The total window [7] can then be calculated from the common window and it can express the image quality in one single number. However, the computation time of the overlapping ED window method is on the order of minutes. This constrains the speed of lithography optimization when large numbers of options must be evaluated. A figure of merit amenable to efficient computation is desirable.

For lithography simulation and computer optimization, we propose the Normalized Process Latitude (NPL) that incorporates these four types of error as one number. This metric takes image sensitivity to dose, focus, aberrations and mask error into consideration and expresses them as a single number that is indicative of the quality of an image. The structure of the NPL consists of three parts: 1) Extraction of the individual sensitivities, 2) Normalization and 3) Combination of individual sensitivities. Extraction of these sensitivities including the normalized image log slope (NILS) [8,9], mask error factor (MEF), focus and aberration sensitivities are first determined. The sigmoid function is then used to normalize these quantities to a range between zero and one. These normalized sensitivities are finally combined into a single number that represents the image quality. Since the NPL does not require computation of the full ED windows, its computation time is within 10 seconds.

---

* h9924945@eee.hku.hk; phone (852)97397739; fax (852)24970240;
** awong@eee.hku.hk; phone (852)28597096; fax (852)25598738

2. EXTRACTION

In this section, we describe how the various sensitivity metrics are extracted. A desirable property of these metrics is that they take into consideration improvements in the fabrication process, i.e., a certain metric value always indicates that the image is robust or not regardless of the critical dimension (CD). In this way, we can obtain an intuitive feeling of the quality of an image. It also allows comparison across generations.

2.1 DOSE SENSITIVITY

The NILS is appropriate for expressing image sensitivity to dose variation:

$$NILS = \left| \frac{CD}{I_{threshold}} \frac{dI}{dx} \Big|_{I_{threshold}} \right| \quad (1)$$

As opposed to the exposure latitude, the NILS is normalized with respect to the CD such that images from different technology generations can be compared.

2.2 MASK ERROR SENSITIVITY

The mask error factor (MEF) is a suitable measure of image sensitivity to mask CD error.

$$MEF = \frac{1}{k} \times \frac{\partial CD_{wafer}}{\partial CD_{reticle}} \quad (2)$$

where k is the reduction ratio

2.3 FOCUS SENSITIVITY

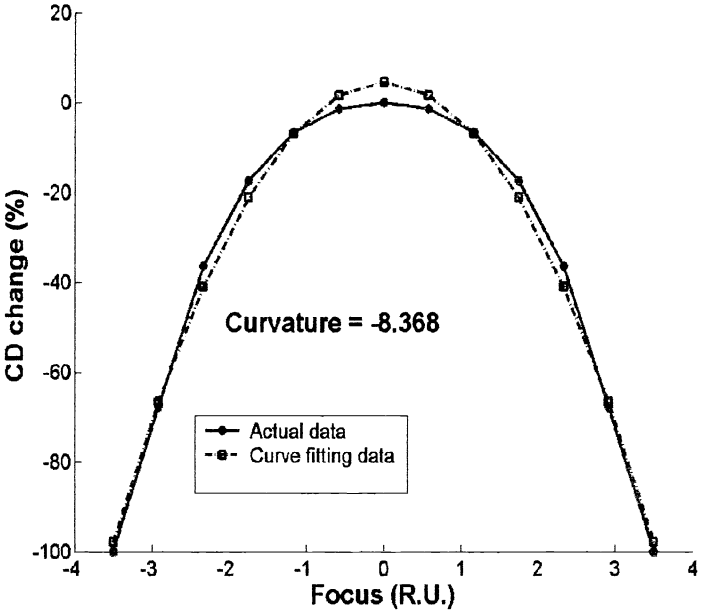

Figure 1: Variation of printed dimension with focus

Depth-of-focus (DOF) has been the traditional measure of focus sensitivity. However, the large number of image computations needed for calculation of the DOF makes it unsuitable for our purpose. If we investigate the dependence of the printed dimension to focus variation, as plotted in Figure 1, we notice that the behavior can be approximated by a second-order polynomial.

The magnitude of the quadratic term coefficient can be used as the measure of CD sensitivity to focus. In so doing, we are neglecting the linear term, an approximation that is acceptable. One point to note is that the focus should be expressed in Rayleigh's unit of depth of focus ($\frac{\lambda}{2NA^2}$) [10] and the CD change should be computed as a percentage to account for technology scaling.

2.4 ABERRATION SENSITIVITY

For low levels of aberration, the change in the printed dimension with increasing amounts of aberration can be considered linear. Figure 2 shows the change in CD with different amounts of spherical aberration, curvature, and distortion.

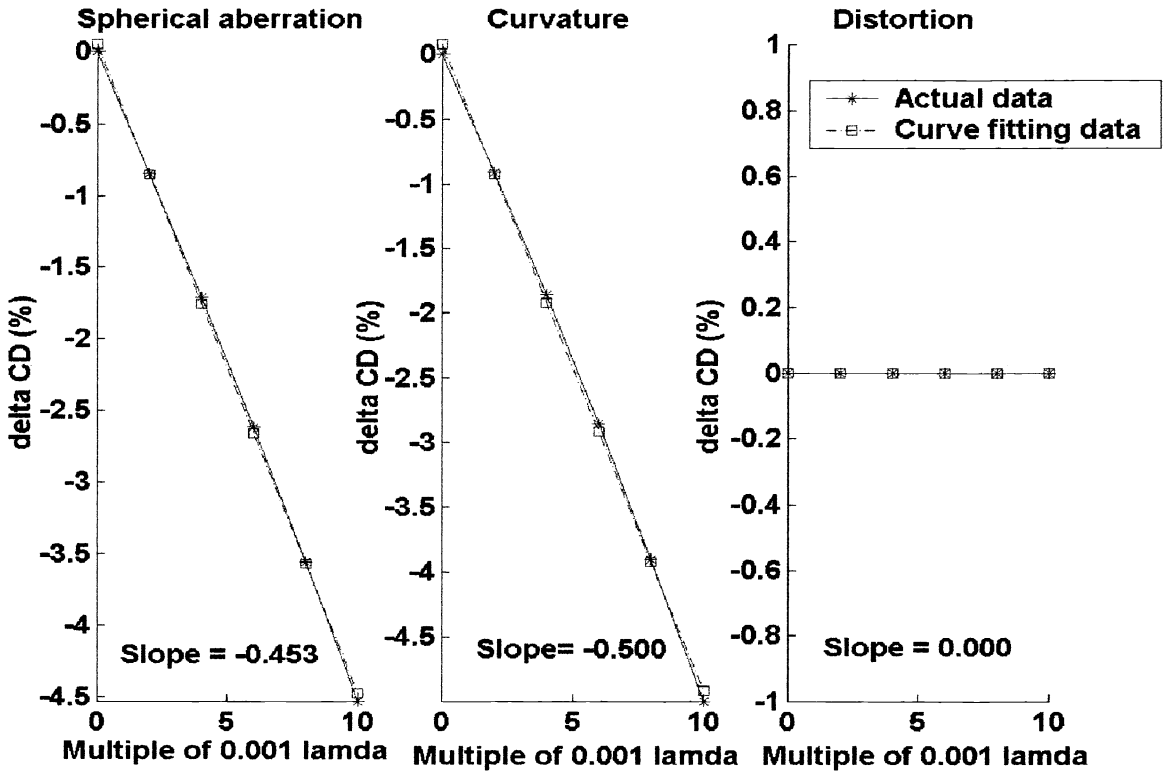

Figure 2: The graph of CD change against aberration (a) Spherical aberration (sa) (b) Curvature (cu) (c) Distortion (di)

The virtual linear dependence means that the sensitivity to a particular aberration can be found by fitting a straight line to the data and extracting the slope. The more sensitive the image, the larger the slope.

To combine the sensitivity to all aberration terms, we propose using the R.S.S. (root of sum of square):

$$S_{aberration} = \sqrt{\sum_{i=1}^{N} S_i^2} \qquad (3)$$

where N is the number of aberration terms considered. In the situation where spherical aberration (sa), coma (co), astigmatism (as), curvature (cu), and distortion (di) are evaluated,

$$S_{aberration} = \sqrt{S_{sa}^2 + S_{co}^2 + S_{as}^2 + S_{cu}^2 + S_{di}^2}$$
$$= \sqrt{(m_{sa})^2 + (m_{co})^2 + (m_{as})^2 + (m_{cu})^2 + (m_{di})^2} \qquad (4)$$

where m is the slope

In our example, the slopes for spherical aberration and curvature are the largest (–0.453 and -0.500 respectively) and they dominate the aberration sensitivity. The metric $S_{aberration}$ reflects this situation. We can conclude that slope is a reasonable metric for measuring sensitivity to aberration.

Note that 1.5 R.U. of focus error is added into the feature to magnify its aberration effect. Otherwise, the influence of aberration on CD will be insignificant.

3. NORMALIZATION

After extracting the sensitivities, we normalize these sensitivities to be within the range of zero and one. Normalization is needed because the values for different kinds of sensitivities are different and they are not directly comparable. After normalization, they all have the same range which can be combined easily. In the mapping of raw metric values to normalized values (we named *robustness*), we would like to discriminate values that impact yield, but we do not necessarily need to differentiate excessively good or poor images by large amounts.
The sigmoid function is a suitable candidate.

Sigmoid function: $$R = \frac{1}{1 + e^{-(\frac{x-c}{\eta})}} \qquad (5)$$

where c is discrimination point and η is spread

In Equation (5), x is the raw metric value, R is the normalized output we named the *robustness*, c is the discrimination point, and η measures how rapidly an image turns from good to poor as the raw metric x varies. These quantities are illustrated in Figure 3.

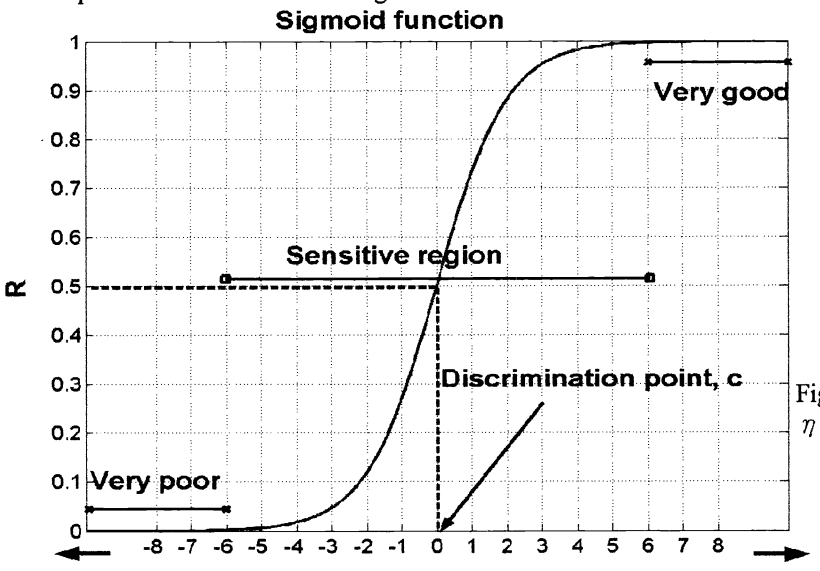

Figure 3: Sigmoid function with c=0 and η =1

To apply the sigmoid function for our normalization, we divide the range of x into 3 regions, namely "very poor", "sensitive" and "very good" regions. Within the "very good" and "very poor" regions, the normalized value is close to 1 and 0 respectively. The output R does not vary much with the input x. In these regions, the image sensitivity is so low or so good that further decrease or increase would not much affect the process. For example, there is not much difference between an image having a NILS of 0.1 and one with a NILS of 0.2; both are equally unusable. In between the "very good" and "very poor" regions is the "sensitive" region. This is the region within which the raw metrics are differentiated. The midpoint of this region is the discrimination point, c. Its value is determined by the user as illustrated in section 5. It can be regarded as the threshold that separates good images from poor ones. The width of the sensitive region is approximately six times the parameter η.

4. COMBINATION

Combination of the individual normalized metrics is accomplished by taking their products, resulting in the normalized process latitude (NPL):

$$NPL = \left(|R_{dose}| \times |R_{mask}| \times |R_{focus}| \times |R_{aberrations}| \right)^{\frac{1}{4}} \qquad (6)$$

where R is robustness of the image with respect to detractor.

The 4th root is taken because we would like a NPL of 0.5 to indicate an average image. For example, if the four individual robustness values are all 0.5. Then the NPL will be 0.5 rather than just $0.5^4 = 0.0625$. Generalization of the NPL to include other types of detractors is straightforward:

$$NPL = \sqrt[N]{\prod_{i=1}^{N} R_i} \qquad (7)$$

Equation (7) indicates that N detractors are considered.
The whole process of NPL calculation is shown in Figure 4.

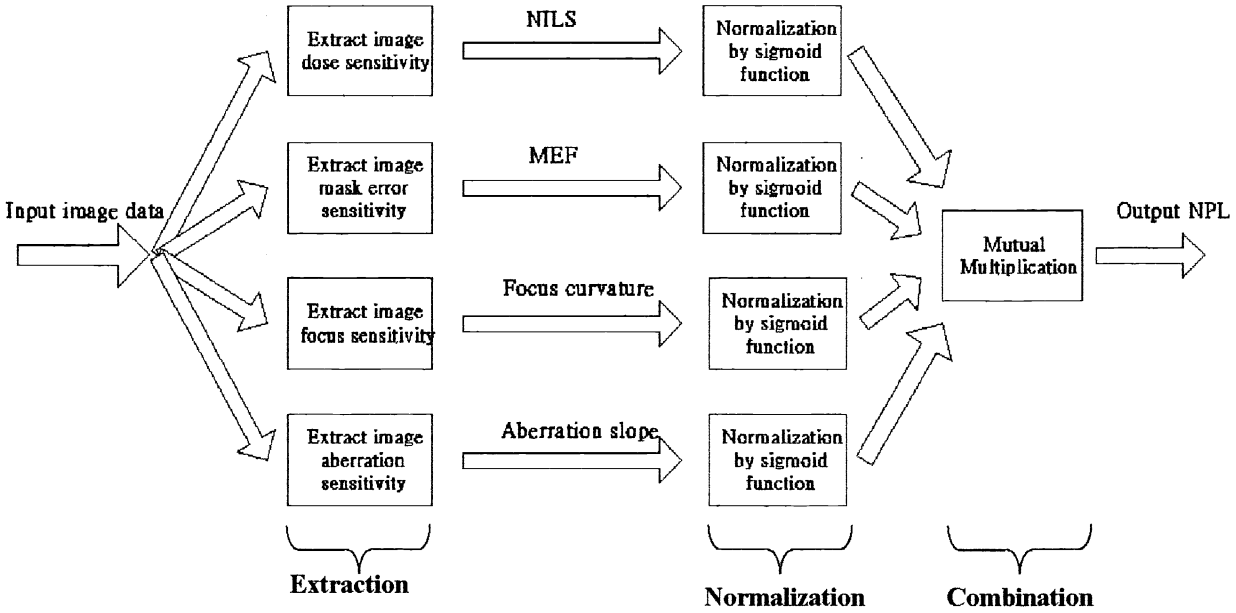

Figure 4: The whole process of NPL calculation

5. APPLICATION EXAMPLE

In order to determine those parameters for normalization, 41 features and their corresponding exposure latitude, depth of focus (DOF), NILS, MEF, focus curvature, and aberration slope are acquired and listed in Table 1. The discrimination point, c, is first roughly determined by the average value of its corresponding sensitivity to be normalized. As for the spread, η, it is determined by finding the difference between the average and the best or worst value of the sensitivity. The spread is then roughly equal to this difference divided by six. These rough values may not be the optimum values. Optimized parameters may be determined by trial and error. Optimum values are obtained when the normalization can discriminate good and poor sensitivity sharply and give similar high value for very good sensitivity and give similar low value for very poor sensitivity. One can also check the NPL with its corresponding total window to see if the normalization gives the right trend.
Several application examples are described to illustrate the correctness of the NPL. The NPL is set up with the following parameters determined from Table 1:

Table 2: The parameters for normalization

Type of sensitivity for normalization	Discrimination point, c	Spread, η
Dose sensitivity	3	0.6
Mask sensitivity	1	0.3
Focus sensitivity	18	1.5
Aberration sensitivity	2	1.5

Table 1: The sensitivities, NPL and total window of the 41 features

Exposure conditions: Wavelength = 0.193um Sigma = 0.8 NA = 0.75

CD (um)	Period (um)	NILS	EL(%)	MEF	DOF (R.U.)	Focus curvature	Aberration slope	NPL	Total window (% R.U.)
0.080	0.176	0.747	3.750	4.161	1.960	18.320	0.917	0.021	5.919
0.080	0.232	1.293	8.400	1.675	1.110	33.730	#	0.005	9.341
0.080	0.288	1.234	7.900	1.803	0.012	78.630	#	0.000	6.466
0.080	0.344	1.258	6.850	1.769	0.012	78.620	#	0.000	5.722
0.080	0.400	1.309	6.750	1.697	0.012	78.490	#	0.000	5.350
0.100	0.220	1.750	13.000	1.587	2.522	18.440	1.055	0.249	24.188
0.100	0.290	2.010	13.500	1.139	1.137	33.700	#	0.010	14.898
0.100	0.360	1.986	11.500	1.214	0.769	33.430	#	0.010	11.785
0.100	0.430	2.414	9.500	1.024	0.681	32.940	#	0.013	8.324
0.100	0.500	2.032	10.000	1.216	0.484	33.230	#	0.010	9.762
0.130	0.286	2.772	22.000	0.927	2.516	18.610	1.269	0.487	39.975
0.130	0.377	2.762	18.000	1.035	1.709	34.150	6.888	0.020	24.052
0.130	0.468	2.875	17.200	0.995	1.509	34.010	15.988	0.005	21.685
0.130	0.559	2.894	17.500	1.012	1.463	33.980	16.033	0.005	21.820
0.130	0.650	2.884	17.000	1.027	1.479	33.980	15.874	0.005	21.958
0.150	0.330	3.256	25.500	0.956	2.407	18.690	1.449	0.522	46.562
0.150	0.435	3.207	21.000	1.007	1.961	19.450	3.384	0.388	30.682
0.150	0.540	3.252	21.500	1.047	1.858	19.950	4.573	0.309	30.604
0.150	0.645	3.290	19.000	1.046	1.884	20.070	4.801	0.296	28.401
0.150	0.750	3.365	19.500	1.054	1.787	20.570	5.367	0.256	30.162
0.180	0.396	3.807	28.000	1.100	2.360	18.550	1.361	0.535	51.093
0.180	0.522	3.944	27.500	1.078	2.023	18.950	2.306	0.487	45.226
0.180	0.648	3.996	25.000	1.086	2.042	18.990	2.464	0.477	41.564
0.180	0.774	4.049	25.000	1.102	2.022	19.010	2.550	0.470	44.087
0.180	0.900	4.096	26.000	1.112	1.912	18.990	2.529	0.471	38.490
0.320	0.576	7.377	49.000	1.025	3.047	8.462	0.408	0.772	141.589
0.320	0.704	7.742	49.500	1.006	2.572	11.610	0.674	0.767	118.662
0.320	0.832	7.915	50.500	1.005	2.588	11.700	0.740	0.764	119.614
0.320	0.960	7.749	50.000	1.027	2.825	11.650	0.680	0.759	124.032
0.400	0.720	9.994	65.500	0.955	2.882	7.821	0.489	0.792	195.921
0.400	0.880	10.180	67.000	0.981	2.678	8.024	0.591	0.780	172.450
0.400	1.040	10.360	68.000	0.994	2.621	8.047	0.601	0.776	175.670
0.400	1.200	10.390	65.500	0.999	2.588	8.020	0.588	0.775	165.490
0.480	0.864	12.060	86.000	0.991	3.025	5.742	0.415	0.783	273.093
0.480	1.056	12.450	84.000	0.986	2.792	5.967	0.474	0.783	244.254
0.480	1.248	12.420	84.000	0.993	2.875	5.888	0.445	0.782	241.590
0.480	1.440	12.290	86.000	0.997	3.002	5.791	0.413	0.781	257.916
0.560	1.008	14.340	103.000	0.967	3.184	4.404	0.374	0.792	368.501
0.560	1.232	14.850	101.000	0.995	2.840	4.628	0.416	0.782	343.127
0.560	1.456	14.730	101.000	0.998	3.015	4.434	0.368	0.783	353.284
0.560	1.680	14.500	101.000	0.998	3.138	4.355	0.351	0.783	366.190

Since its depth of focus is too small, its aberration effect is not considered.

In the examples with overlapping window, the mask error window is of ±1% and the aberration error window is of 0.005λ aberration.

5.1 VERY SMALL OVERLAPPING WINDOW AND THE NPL

Feature	0.08um line
Mask	COG mask
Wavelength	0.193um
NA	0.75
Sigma	0.8
Period	2.2 x CD
Mask error	±1%

Table 3: Feature information for example 5.1

In this example, we compare a case with a very small overlapping window with the NPL. The resulting NPL has the following parameters:

Table 4: The parameters of the resulting NPL

NILS	0.747
MEF	4.16
Focus curvature	18.3
Aberration slope	0.917

Robustness of NILS	0.0229
Robustness of MEF	0.00003
Robustness of focus curvature	0.447
Robustness of aberration slope	0.673

Table 5: The quantification results

NPL	0.00207
Total window	5.89% R.U.

In this situation, the mask error factor is high and the overlapping total window is 5.89%R.U.
So, the results of the total window and the NPL agree with each other.
The ED (exposure-defocus) windows for this example are shown in Figure 5:

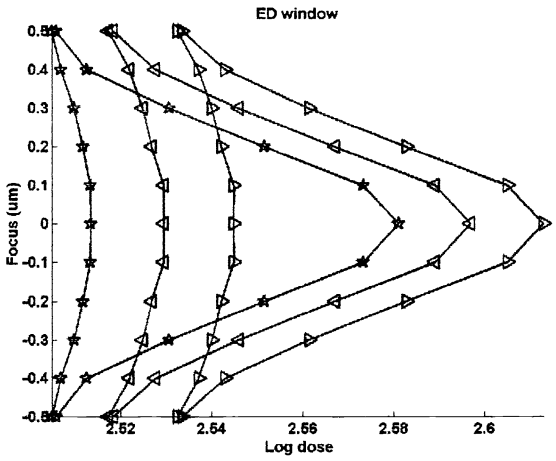

Figure 5: The ED windows for normal situation, with +1% mask error and –1% mask error

Normal ——— ◁

+1% mask error ——— ▷

-1% mask error ——— ☆

5.2 COMPARING BIGGER AND SMALLER CDS

Table 6: Feature information for example 5.2

Feature	0.08um line	0.18um line
Mask	COG mask	COG mask
Wavelength	0.193um	0.193um
NA	0.75	0.75
Sigma	0.8	0.8
Period	2.9 x CD	2.9 x CD
NILS	1.29	3.94
MEF	1.68	1.08
Focus curvature	33.7	19.0
Aberration slope	10	2.31
Robustness of NILS	0.0549	0.828
Robustness of MEF	0.0953	0.435
Robustness of focus curvature	0.0000279	0.347
Robustness of aberration slope	0.00480	0.449
NPL	0.0051	0.487
Total window	9.34% R.U.	45.2% R.U.

The overlapping window of the 1st feature is shown below:

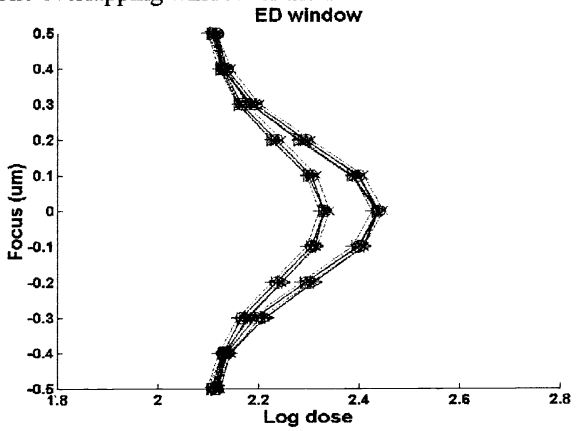

Figure 6: The ED windows of normal, mask errors, and aberrations together form an overlapping common window for the 1st feature

The overlapping window of the 2nd feature is also shown:

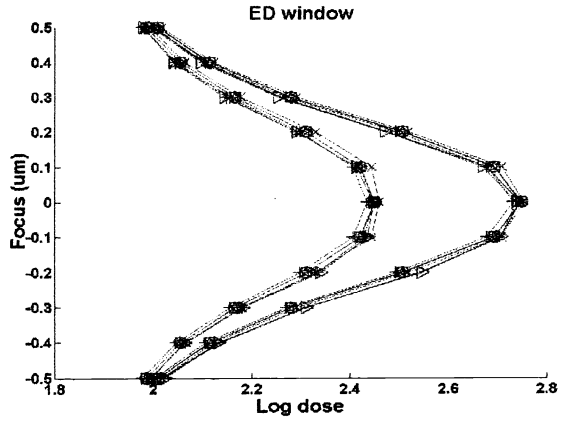

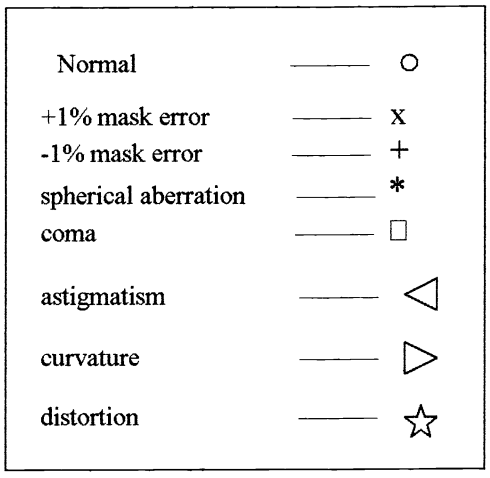

Figure 7: The ED windows of normal, mask errors, and aberrations together form an overlapping common window for the 2nd feature

COMPARISON OF RESULTS FOR THE FEATURES OF TABLE 1

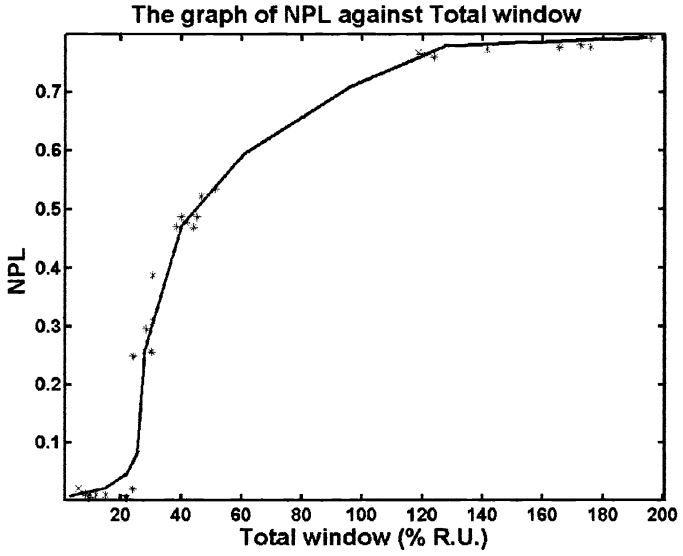

Figure 8 indicates the difference between NPL and total window method. In NPL, for very poor or very good images, their quantification results do not vary much with qualities. However, for total window, as long as image quality improves or goes worse, its value will keep on increasing or decreasing without limit.

Figure 8: The graph of NPL against total window for the features in Table 1

5.3 CONTOUR PLOTS FOR TOTAL WINDOW AND NPL OF VERY GOOD IMAGES

The total window and NPL as functions of CD and pitch are compared in Figure 9 and 10 respectively. Within the figures, the CD ranges from 0.32 um to 0.56um, while the period varies from 1.8 x CD to 3.0 x CD. Their exposure conditions are wavelength = 0.193um, sigma = 0.8, and NA=0.75. Figure 9 shows the total window of the images. In general, the total window increases with the CD, from a normalized value of 0.32 to 1. Since the CDs of these features are large (k_1 ranges from 1.24 to 2.18), these images have very good qualities and we expect that their NPLs are close to 1. This is the situation shown in Figure 10. Notice that the color scale in Figure 10 is different from that in Figure 9. The range of the color bar of the total window is much wider that that of the NPL since the variation within the contour plot of the total window is much larger than that of the NPL. The trend in the NPL is not as fast as that of the total window because the NPL method gives similar quantification results for very good images while the total window method will give better result as long as the image quality goes on improving.
Figure 9 and Figure 10 show the contour plots of the total window and NPL of the 16 features.

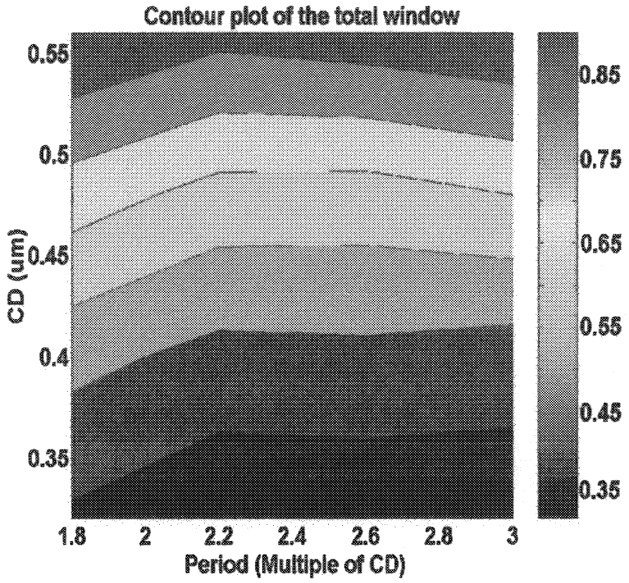

Figure 9: Total window as functions of CD and period

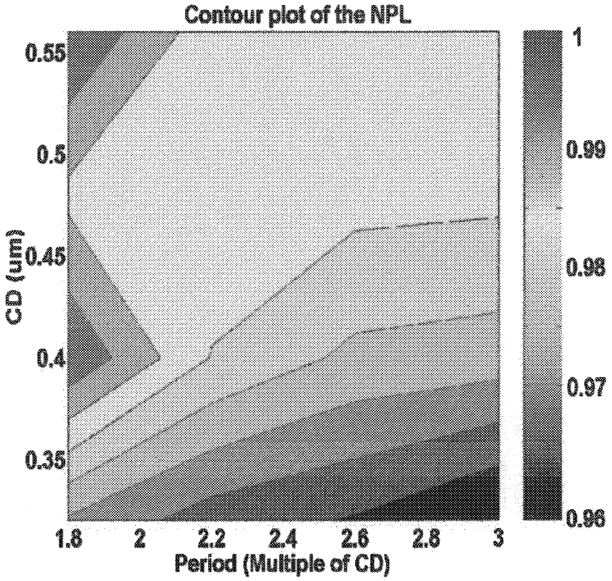

Figure 10: NPL as functions of CD and period

6. CONCLUSION

In this paper, a new metric called "Normalized Process Latitude (NPL)" is proposed. Its computation time is within 10s and it is generally 10 times faster than the traditional overlapping window metric. The formation and the structure of the NPL are discussed and application examples are provided to illustrate and verify the usefulness and correctness of this new metric. It is shown that the total window method and the NPL give similar quantification results for the example features and thus the NPL is a sensible figure of merit for image quality quantification. The adjustable parameters in the model can be adjusted by the user based on process information.

7. REFERENCES

[1] H.Y. Liu, C. Yu, and R. Gleason, "Contributions of stepper lenses to systematic CD errors within exposure fields," in *Proc.SPIE* (T. Brunner, ed.), vol. 2440, pp. 868--877, 1995.

[2] A. Wong, R. Ferguson, L. Liebmann, S. Mansfield, A. Molless, and M. Neisser, "Lithographic effects of mask critical dimension error," in *Proc. SPIE* (L. van den Hove, ed.), vol. 3334, pp. 106--116, 1998.

[3] R. Schenker, "Effects of phase shift masks on across field linewidth control," in *Proc.SPIE* (L. van den Hove, ed.), vol. 3679, pp. 18--26, 1999.

[4] B. J. Lin, "Partially coherent imaging in two-dimensions and theoretical limits of projection printing in microfabrication," *IEEE Transactions on Electron Devices*, vol. 27, pp. 931--938, May 1980.

[5] B. J. Lin, "Methods to print optical images at low-k_1 factors," in *Proc. SPIE* (V. Pol, ed.), vol. 1264, pp. 2--13, 1990.

[6] R. Ferguson, R. Martino, and T. Brunner, "Data analysis methods for evaluating lithographic performance," *J. Vac. Sci. Technol. B*, vol. 15, pp. 2387--2393, Nov. 1997.

[7] A. Wong, R. Ferguson, S. Mansfield, A. Molless, D. Samuels, R. Schuster, and A. Thomas, "Level-specific lithography optimization for 1Gb DRAM," *IEEE Transactions on Semiconductor Manufacturing*, vol. 13, pp. 76--87, Feb. 2000.

[8] M. D. Levenson, "The phase-shifting mask II: Imaging simulations and submicrometer resist exposures," *IEEE Transactions on Electron Devices*, vol. 31, pp. 753--763, June 1984.

[9] C. A. Mack, "Understanding focus effects in submicron optical lithography," in *Proc. SPIE*, vol. 922, pp. 135--148, 1988.

[10] M. Born and E. Wolf, *Principles of Optics*, section 9.3, pp.~468--473. Pergamon Press, sixth ed., 1980.